ELSEVIER

Chemical Engineering Journal 74 (1999) 43–56

Chemical Engineering Journal

Modeling tracer counter-permeation through anisotropic zeolite membranes: from mean field theory to single-file diffusion

Peter H. Nelson[a], Scott M. Auerbach[a,b,*]

[a]*Department of Chemistry, University of Massachusetts, Amherst, MA 01003, USA*
[b]*Department of Chemical Engineering, University of Massachusetts, Amherst, MA 01003, USA*

Abstract

Diffusion in anisotropic host–guest systems exhibiting a Langmuir-type adsorption isotherm is investigated using a tracer counter-permeation (TCP) simulation technique. In the TCP simulations, tagged and untagged molecules counter-diffuse through zeolite membranes of finite thickness. Fick's law is used to measure the diffusivities at high equilibrium occupancy, as a function of the membrane thickness, L, and anisotropy, η. For values of $\eta \gg 1$, sorbate motion in the plane of the membrane is very rapid and washes out any correlations in the transmembrane direction, so that diffusion is well modeled by mean field theory. As η is reduced, correlations between the motion of nearby molecules decrease the counter-diffusivity, but diffusion remains ''normal'' in the sense that the diffusivity is independent of thickness for sufficiently thick membranes. For membranes with $\eta=0$, a single-file mode of diffusion occurs for all membrane thicknesses, and the counter-diffusivity becomes inversely proportional to thickness for thick membranes. Membranes with $\eta \ll 1$ exhibit a single-file diffusion mode for thin membranes that changes over to a normal diffusion mode as the thickness is increased. We have also determined that the rate of transmembrane permeation is controlled by the ratio of the diffusion time to the sorption time, which is given by $k_d L/D$ where D is the counter-diffusivity and k_d is the desorption coefficient. When permeation is diffusion limited, an assumption of local thermodynamic equilibrium is appropriate at the edges, and the permeability coefficient is independent of membrane thickness. On the other hand, when permeation is sorption limited, the edge concentrations are not determined by the isotherm, and the permeability coefficient depends on thickness so that the permeance is itself independent of membrane thickness.

Keywords: Counter-permeation; Anisotropic zeolite membranes; Mean field theory; Single-file diffusion; Kinetic Monte-Carlo

1. Introduction

The transport properties of adsorbed molecules play a central role in zeolite-based separations and catalysis [1–3]. Although computational studies have greatly enhanced our understanding of self-diffusion in zeolites [4,5], very few have modeled transport diffusion [6–11], which arises from a non-equilibrium chemical potential gradient, and is the process most relevant to industrial applications. Modeling transport diffusion in zeolite membranes is of increasing practical importance because of recent progress in synthesizing continuous zeolite membranes [12–15]. In this paper, we report diffusion theory and kinetic Monte-Carlo simulations of transport diffusion through model zeolite membranes, to explore how permeation is controlled by microscopic and macroscopic system parameters.

Permeation through zeolite membranes is controlled by several factors, including membrane thickness and continuity, zeolite framework topology and alignment, intra- and extra-crystalline molecular jump rates and heats of adsorption, temperature, and external driving forces such as composition and concentration gradients. Although our eventual goal is to include as many of these effects as possible, including too many at once will make it difficult to determine which aspects of the model are essential to the theory and simulation results. In this article, we focus on how membrane thickness, molecular jump rates, and heats of adsorption affect membrane permeation.

In order to determine the relative importance of these factors, and to keep the simulations tractable, we begin by modeling a simple zeolite membrane composed of a two-dimensional square lattice of identical adsorption sites, of finite extent in the transmembrane direction, and having periodic boundary conditions in the other direction. We also assume that site occupation numbers are either zero or one,

*Corresponding author. Tel.: +1-413-545-1240; fax: +1-413-545-4490; e-mail: auerbach@chem.umass.edu

1385-8947/99/$ – see front matter
PII: S1385-8947(99)00052-2

and that sorbates do not otherwise interact with each other. In future work, we will consider more complicated lattice structures and sorbate–sorbate interactions, to determine the importance of these additional factors.

The lattice described above has special adsorption and diffusion properties, making it a good starting point for further development of membrane permeation models. Indeed, it is straightforward to show that our present model gives a Langmuir adsorption isotherm [16]. For that reason, we refer to host–guest systems that are well represented by this model as "Langmuirian." The transport diffusion coefficient for this lattice model can be defined by Fick's law, $J=-D\nabla\theta$, where J is the net flux through a surface, D is the transport diffusivity, and $\nabla\theta$ is the local concentration gradient perpendicular to the surface. The concentration dependence of D is of special interest, and is usually discussed in terms of the Darken equation [1,9],

$$D = D_{\mathrm{C}}\left(\frac{\partial \ln f}{\partial \ln \theta}\right)_T, \tag{1}$$

where D_{C} is the so-called corrected diffusivity, f the fugacity of the external fluid phase, θ the intra-crystalline sorbate concentration, and T is the temperature. The Darken equation is especially useful when the corrected diffusivity is nearly independent of occupancy, so that the concentration dependence of the transport diffusivity is controlled by the thermodynamic factor. It is well known, however, that the single-component transport diffusivity in Langmuirian host–guest systems is itself independent of concentration [7,17], rendering the corrected diffusivity less useful in this case. For this reason, we focus on calculating the transport diffusivity from Fick's law, to investigate the factors controlling zeolite membrane permeation.

Diffusion anisotropy in zeolites results from molecular jump rates that depend upon direction [18,19]. Diffusion anisotropy takes on special importance for permeation through oriented zeolite membranes, because the anisotropy introduced by a transmembrane concentration gradient can couple with the anisotropy inherent in a zeolite–sorbate system, yielding novel transport properties. In our two-dimensional lattice model, anisotropy leads to single-file transport through the membrane at one extreme, and single-file transport in the plane of the membrane in the other extreme. Although single-file motion at finite loadings exhibits normal concentration-independent, single-component transport diffusion, single-file motion gives rise to anomalous self-diffusion, wherein the mean-square displacement (MSD) scales at long times as $\sqrt{t}$ rather than t [20,21]. It is therefore of interest to investigate the signature of such anomalous self-diffusion in a membrane transport system. However, since the long time limit of the MSD may not be accessible in a membrane of finite thickness, and since the natural observable in a permeation measurement is steady-state flux rather than the MSD, we need to imagine a convenient experiment that can probe this anomalous diffusion. Indeed, it has been shown that two-component, equimolar counter-permeation of identical, labeled species yields transport identical to self-diffusion [8]. Such a situation is closely related to the tracer zero-length column experiment developed by Ruthven and co-workers [22].

In this paper, we will examine how extreme diffusion anisotropy produces anomalous transport through zeolite membranes of various thicknesses, by performing tracer counter-permeation (TCP) computer experiments. Fick's law is applied directly to determine the counter-diffusivities under steady-state conditions. We find that the counter-diffusivity is independent of membrane thickness in all cases that are not strictly single-file, as long as the membrane is sufficiently thick. When the diffusion anisotropy favors motion normal to the transmembrane direction, we find that mean field theories of diffusion are quantitatively accurate; while in the other case we find the signature of anomalous diffusion, namely that the counter-diffusivity scales inversely with the membrane thickness [23,24].

The remainder of this paper is organized as follows: in Section 2 we review the theory of two-component tracer diffusion; in Section 3 we describe how we model the membrane transport system; in Section 4 we discuss the details of the simulation method; in Section 5 we detail the results of the simulations; in Section 6 we discuss our findings; and in Section 7 we give concluding remarks for future work.

2. Diffusion theory

2.1. Langmuirian host–guest systems

In this paper, we investigate host–guest systems with a Langmuir adsorption isotherm. Such a system is shown schematically in Figs. 1 and 2. The basic requirement for a host–guest system to be "Langmuirian" is that the host has a periodic array of identical adsorption sites that may contain at the most one guest molecule. The adsorption sites are represented as squares in Fig. 1 and energy minima in Fig. 2. The differential heat of adsorption is independent of sorbate loading up to a fractional occupancy of $\theta=1$, i.e. the sites are energetically uncoupled from each other. It is also assumed that diffusion proceeds by a sequence of thermally activated jumps, in which a sorbate molecule jumps from one site to a vacant nearest neighbor site, only after overcoming an energy barrier of E_x in the x-direction (see Fig. 2). Attempted jumps to occupied sites are unsuccessful because double occupancy is forbidden.

A Langmuirian host–guest system exposed to a fluid will have an adsorption isotherm of the form:

$$\theta_{\mathrm{eq}} = \frac{1}{1 + (k_{\mathrm{d}}/\nu)}, \tag{2}$$

where θ_{eq} is the equilibrium occupancy, which is uniform throughout the system and k_{d} is the rate coefficient for

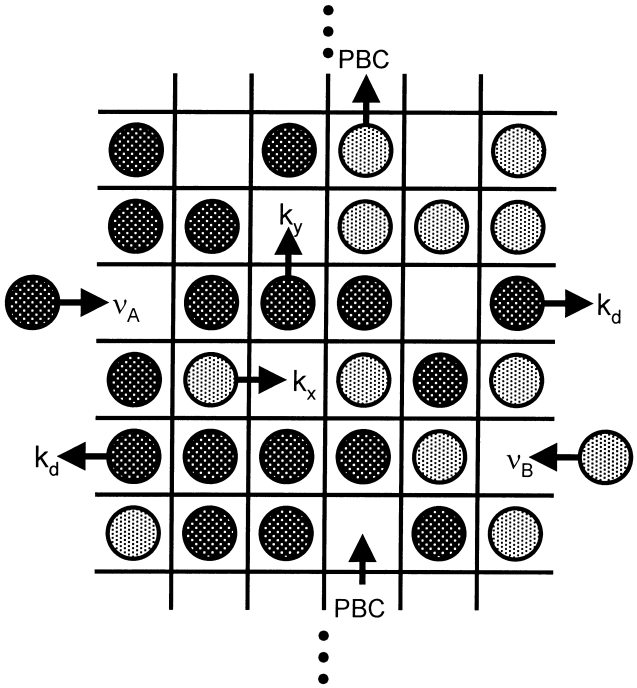

Fig. 1. Schematic representation of a Langmuirian zeolite membrane with tracer counter-permeation (TCP) boundary conditions. Differently labeled particles move through the membrane with the same rates: k_x and k_y for jumps in the x- and y-directions, and k_d for jumps out of the lattice. Constant chemical potentials of components A (darker circles) and B (lighter circles) are maintained by adsorption rates v_A and v_B at the left and right edges, respectively. Periodic boundary conditions are maintained in the y-direction.

desorption, via thermally activated hops of a molecule located in an edge site to the fluid phase. v is the rate of insertion attempts of molecules from the fluid phase into each exposed adsorption site at the edge of the zeolite. Eq. (2) is derived by equating the rate of actual insertion, $v(1-\theta_{eq})$, and the rate of desorption, $k_d\theta_{eq}$, at equilibrium. Because our goal is a kinetic transport study, this kinetic form of the Langmuir isotherm is most relevant to the systems under consideration here. For an isothermal ideal gas, v is proportional to the gas pressure, and the more usual form of the Langmuir isotherm is recovered:

$$\theta_{eq} = \frac{1}{1+(b/p)}, \tag{3}$$

wherein occupancy is given as a function of the pressure, p.

Transport diffusion of a single component in a Langmuirian host–guest system is consistent with Fick's law for all simple lattices [7,17,25]:

$$J = -D\nabla\theta, \tag{4}$$

where J is the net particle flux (number per unit area per unit time) and $\nabla\theta$ is the occupancy gradient in a non-equilibrium system. For the system shown in Fig. 1, $\nabla\theta$ is defined as $\nabla\theta \equiv (\theta_{n+1}-\theta_n)/\Delta x$, where θ_n is the occupancy of column n, and $\Delta x \equiv 1$ is the distance between adjacent columns. The transport diffusion coefficient, D, is independent of occupancy [17,25], position and concentration gradient [7]. At first glance this result is quite surprising, since the effective jump rate for a given molecule depends strongly on concentration, being of the form $k_x(1-\theta)$ within the mean field approximation, where k_x is the jump rate coefficient. A simple explanation of this result [26] is that the reduction in the actual flux of particles from one lattice site to another is compensated by an equal reduction in the actual flux in the opposite direction, so that the net flux is unaffected by the exclusion of double occupancy.

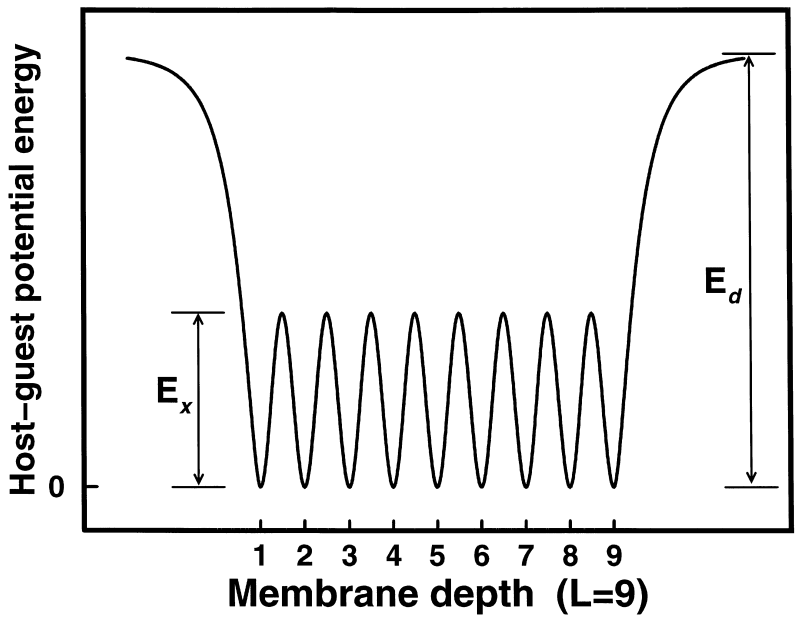

Fig. 2. Schematic representation of the Langmuirian host–guest potential energy in the x-direction. Adsorption sites (minima) are separated by an energy barrier of E_x. Desorption from an edge site requires energy E_d. Double occupancy is forbidden, but otherwise guests do not interact with each other.

This simple Langmuirian host–guest model appears to be an excellent approximation for several important zeolite–sorbate systems. A typical example is cyclohexane in silicalite, where experimental results are consistent with the Langmuirian model up to a maximum loading of four molecules per unit cell [19]. Specifically, the adsorption isotherm is Langmuirian, and the differential heat of adsorption and single-component transport diffusion coefficient are found to be nearly independent of sorbate loading. This should be expected because the channel intersections, where cyclohexane is adsorbed, are separated by a relatively large distance, so that the molecules in adjacent sites do not interact strongly.

Silicalite–sorbate systems that involve smaller sorbate molecules, which preferentially adsorb in the eight channel segments between intersections in the silicalite unit cell, can also be modeled as Langmuirian host–guest systems for the first step of the isotherm, provided that there is no significant occupation of other adsorption sites. In this case, the Langmuirian occupancy, θ, must be expressed as a fractional occupancy of the most stable sites. In molecular dynamics simulations of methane in silicalite, the transport diffusivities were found to be independent of loading, up to a loading of nearly eight methane molecules per unit cell [9]. This concentration-independent, single-component transport diffusivity in silicalite has also been observed experimentally for a number of sorbate molecules, including: methane, ethane, propane, *n*-butane, *n*-pentane and isobutane [27,28];, benzene, toluene, and 2-methylbutane [29–31]; and cyclohexane, methylcyclohexane, and ethylcyclohexane [19].

2.2. Matrix formulation of diffusion

As mentioned in the introduction, we wish to investigate two-component transport diffusion in an anisotropic membrane. The theory for the corresponding isotropic membrane has been reported previously [8], and can be used for the anisotropic membranes investigated herein. We define the spatially and temporally varying occupancies of the components A and B, co-adsorbed in a Langmuirian membrane as follows: $\theta_{A,n}(t)$ is the number of lattice sites filled with A-particles at time t in column n, divided by the number of sites in column n; $\theta_{B,n}(t)$ is defined similarly for *B*-particles. $\theta_{T,n}(t)$ is the total fractional occupancy of column n at time t, defined as $\theta_{T,n}(t)=\theta_{A,n}(t)+\theta_{B,n}(t)$. In what follows, we will omit the explicit dependence on column n and time t, e.g. $\theta_{A,n}(t)\rightarrow\theta_A$, unless clarity requires otherwise.

It is well established that the scalar form of Fick's law should be replaced by a vector equation of the form [2,8,25,32,33]:

$$\begin{pmatrix} J_A \\ J_B \end{pmatrix} = -\begin{pmatrix} D_{AA} & D_{AB} \\ D_{BA} & D_{BB} \end{pmatrix}\begin{pmatrix} \nabla\theta_A \\ \nabla\theta_B \end{pmatrix}, \tag{5}$$

where species A and B have *identical* diffusive properties. The diffusion matrix (5) is asymmetric and has two eigenvectors that correspond to the two eigenmodes of diffusion for differently labeled, identical particles. The co-diffusion eigenmode has A and B diffusing together, with driving forces proportional to their occupancies, so that the labeling of the particles does not affect their transport. In this eigenmode the flux of component A can be written in a scalar form of Fick's law:

$$J_A = -D_A^+\nabla\theta_A, \tag{6}$$

and likewise for component *B*. The apparent diffusivities, D_A^+, for the co-diffusion eigenmode are given by:

$$D_A^+ = D_B^+ = D_0, \tag{7}$$

where D_0 is the single-component transport diffusivity which is independent of loading. Thus, the two components diffuse together as if the other component were not present.

The other eigenmode corresponds to equimolar counter-diffusion, where the flux of A is equal and opposite to the flux of B at constant θ_T, so that

$$\nabla\theta_B = -\nabla\theta_A. \tag{8}$$

The apparent diffusivities (6) for counter-diffusion are given by

$$D_A^+ = D_B^+ = D_0(1-\theta_T)f(\theta_T) = D_S(\theta_T), \tag{9}$$

where $f(\theta_T)$ is the so-called correlation factor. Eq. (9) shows that the apparent diffusivities arising from equimolar counter-diffusion are identical to the self-diffusion coefficient, D_S. D_0 is the single-component transport diffusivity, and is also the self-diffusion coefficient at infinite dilution; i.e. where all jump attempts are successful. $(1-\theta_T)$ is the fraction of initial jumps that are successful because they are directed towards a vacancy. Immediately after a successful jump there is always a vacancy at the particle's original position. The increased probability of the particle returning to its original position is accounted for by the correlation factor f, which is less than one.

In mean field theory, the correlations between successive jumps of a particle are ignored, making the correlation factor equal to unity. This approximation is valid at low loadings, where each particle is likely to be surrounded by vacancies. At high loadings, the correlations between successive jumps reduce the self-diffusivity by the factor f. The theory of correlated motion on anisotropic square lattices of Tahir-Kheli and El-Meshad [34] is directly applicable to our study, and will be used below. For brevity, we do not reproduce their theory here.

Eq. (9) demonstrates the correspondence between self-diffusion and the transport diffusivity measured during tracer counter-permeation (TCP). This theory is a special case of the more general theory presented by Kehr et al. [25], based on an Onsager formalism that was devised for diffusion in a lattice-gas model of a two-component alloy. In what follows, we will investigate the effect of lattice anisotropy and finite system size on the correlation factor, $f(\theta_T)$.

2.3. Finite difference formulation of diffusion

The kinetic theory for sorption and diffusion in a Langmuirian host–guest system is based on a finite difference formulation of diffusion [8], which we briefly describe below. The nodes in the finite difference formulation have the physical meaning of being adsorption sites. Hence the grid spacing in the finite difference formulation is the distance between sites, Δx. For two-component diffusion in the interior of the lattice, we can write [8]:

$$\frac{\delta\vec{\theta}_n}{\delta t} = \underline{\underline{D}}(\langle\theta_T(n, n-1)\rangle)(\vec{\theta}_{n-1} - \vec{\theta}_n) - \underline{\underline{D}}(\langle\theta_T(n, n+1)\rangle)(\vec{\theta}_n - \vec{\theta}_{n+1}), \quad (10)$$

and we can write:

$$\frac{\delta\vec{\theta}_1}{\delta t} = \begin{pmatrix} v_A(1-\theta_{T,1}) - k_d\theta_{A,1} \\ -k_d\theta_{B,1} \end{pmatrix} - \underline{\underline{D}}(\langle\theta_T(1,2)\rangle)(\vec{\theta}_1 - \vec{\theta}_2) \quad (11)$$

for column 1 with a similar equation for column L. The diffusion matrix, $\underline{\underline{D}}$, is evaluated using a concentration, $\langle\theta_T(m,n)\rangle$, that is averaged between adjacent columns m and n.

3. Model membrane system

Consider a lattice membrane as shown in Fig. 1. The adsorption sites are shown as square regions that may contain either an A-particle or a B-particle, or may be vacant. Each site can contain at the most one particle so that double occupancy is rigorously excluded. The A and B particles are distinguishable by, e.g. isotopic labeling, but are otherwise identical in terms of their transport properties. The lattice model and boundary conditions follow those used previously for isotropic zeolite membranes [8].

In the simulations reported here, the lattice is initially empty (at t=0), and particles are introduced into the lattice (t>0) by particle insertions into the edge columns of the lattice. These particle insertion attempts are made at a constant rate per edge site, but in accordance with the exclusion of double occupancy condition, only particle insertion attempts into empty lattice sites are successful. Insertion attempts into an already occupied lattice site result in no net change in the configuration of the lattice. The left-hand edge of the lattice is exposed to an infinite reservoir of A-particles at constant chemical potential, while the right-hand edge is exposed to an infinite reservoir of B-particles at constant chemical potential. The constant chemical potential boundary condition at the left-hand side is maintained by a constant rate, v_A of A-particle insertions per vacant edge site. The boundary condition on the right-hand side is maintained similarly by B-particle insertions at rate v_B. Particles desorb from the edges into the reservoir with a rate coefficient k_d. Once a particle desorbs into the infinite reservoir, it has zero probability of returning. In the systems discussed here, the rate coefficient, k_d, is the same for both A and B particle types because they are assumed to have identical properties, except for being labeled.

Transport throughout the lattice is achieved by particle jump attempts from one site to an adjacent site with the rates k_x and k_y, in the x- and y-directions, respectively. We define the anisotropy parameter, η, as being the ratio

$$\eta = \frac{k_y}{k_x} \quad (12)$$

of the attempted jump rates in the y- and x-directions. η=1 corresponds to an isotropic lattice, η>1 corresponds to a membrane where the jump rate in the transmembrane direction is slower, and η<1 corresponds to a membrane where diffusion is faster in the transmembrane direction. The limiting case η=0 corresponds to single-file diffusion.

In accordance with the requirement that double occupancy must be excluded, only attempted particle jumps toward a vacant site are successful, so that attempted jumps towards an occupied site result in no actual change in the system configuration. The top and bottom edges of the lattice are connected together using periodic boundary conditions, so that a particle that jumps upwards from the top row appears in the bottom row as indicated in Fig. 1.

Fig. 2 shows a schematic energy diagram for the guest molecules as a function of position in the host lattice. In going from a position outside of the lattice to an adsorption site inside the lattice, the molecules energy is lowered by an amount E_d, which is the energy of adsorption. At this level of theory, we assume that the rate at which A-molecules enter an empty site from the fluid phase is determined by the frequency v_A, i.e. the frequency with which molecules from the external phase strike the zeolite with a trajectory that leads to adsorption. For an external, ideal gas phase, this frequency is proportional to the collision frequency of molecules with a plane of unit area in the gas phase. Hence, for low pressure gas phases, the frequency is proportional to the pressure in isothermal systems, and from the kinetic theory of gases we have the more general result that:

$$v_A = \alpha_1\rho_{gas}\sqrt{T}, \quad (13)$$

where α_1 is a prefactor determined by the surface topology of the zeolite and the mass of the molecule, ρ_{gas} the gas phase density and T is the absolute temperature. The rate coefficient for desorption of a molecule in an edge site to the external phase is given by

$$k_d = \alpha_2\exp(-\beta E_d), \quad (14)$$

where β=1/$k_B$$T$, k_B is Boltzmann's constant, and we have assumed that the exit of the molecule from the lattice is a thermally activated process with an activation energy given by the heat of adsorption. The rate at which a particle hops from one adsorption site to an adjacent adsorption site in the

x- and y-directions are given by

$$k_x = \alpha_3 \exp(-\beta E_x) \quad \text{and} \quad k_y = \alpha_4 \exp(-\beta E_y), \tag{15}$$

where E_x and E_y are the activation energies for jumping between two adjacent sites in the x- and y-directions, respectively. The processes governed by the rates k_x, k_y, k_d, ν_A, and ν_B are assumed to be independent Poisson processes with an instantaneous probability that is Markovian, i.e. the probability only depends on the current state of the system, and does not depend the system's history.

4. TCP simulation method

In this paper we are primarily interested in the properties of host–guest systems at high fractional occupancies, e.g. θ_T=0.9. It is at high occupancy that the effects of correlations are most significant, and the counter-diffusion eigenmode is significantly different from the co-diffusion eigenmode. In the simulations reported here, we use a vacancy algorithm [25,35,36] wherein a particle-vacancy pair is chosen by looking first for the vacancy. The approach of [7,8] may be called a "particle method," as the vacancy-particle pair is found by first selecting a particle. The particle method becomes most efficient at low particle concentrations, while the vacancy method is most efficient at low vacancy concentrations. At intermediate concentrations, a process list [37] could be used to eliminate unsuccessful jump attempts from the simulation scheme. The advantage of the vacancy algorithm is its simplicity, since only a list of the vacancy coordinates needs to be maintained in the simulation.

All distinct types of events, i.e. events with the same rate, that occur in the model system must be identified [7]. There are three distinct types of vacancies in our simulations, determined by whether they are in the bulk of the lattice (columns 2 to $L-1$), in the left edge column of sites (column 1), or the right edge column of sites (column L). For vacancies in the bulk of the lattice, there are two types of events that can occur. These are the attempted exchanges of a selected vacancy with a particle in the x- or y-directions. If there are N_b vacancies in the bulk of the lattice, these two event types, (i) and (ii), occur with a total rate of $2k_xN_b$ and $2k_yN_b$ for attempted particle exchanges in the x- and y-directions, respectively. The factor of 2 arises because either positive or negative particle displacement attempts occur at the same rate.

There are eight other types of events that can occur in the simulation, four each for columns 1 and L. In column 1 there are M sites containing N_1 vacancies and $M-N_1$particles, and the event rates are: (iii) $2k_yN_1$ – for attempted vacancy moves in either the positive or negative vertical direction; (iv) k_xN_1 – for attempted vacancy exchange with a particle in column 2; (v) ν_AN_1 – for A-particle insertion into a vacant site in column 1; and (vi) k_dM – for attempted particle desorption from column 1.

In event types (iii) through (v) a vacancy in column 1 is selected first. Event type (vi) is a particle-type move, as one of the M sites in column 1 is selected first, and if that site contains a particle, it desorbs from the lattice and is replaced by a new vacancy. If the site contains a vacancy, the time variable is incremented but there is no change in the system configuration. At the right hand edge, the four event types are: (vii) $2k_yN_L$ – for attempted vacancy moves in either the positive or negative vertical direction; (viii) k_xN_L – for attempted vacancy exchange with a particle in column $L-1$; (ix) ν_BN_L – for B-particle insertion into a vacant site in column L; and (x) k_dM – for attempted particle desorption from column L.

We coordinate the events as follows [7]. There are at most j=10 independent event types that can occur in the simulation with an total instantaneous rate of

$$k_{tot} = \sum_{i=1}^{j} k_i, \tag{16}$$

so that the mean time elapsed before the next event is given by $1/k_{tot}$, and the probability that the next event is of type i is given by

$$P_i = \frac{k_i}{k_{tot}}. \tag{17}$$

We are able to use the average inter-event time $1/k_{tot}$ rather than a number taken from the distribution, $P_{int} = k_{tot}\, e^{-k_{tot}t}$, because $1/k_{tot} \ll 1/k_x$ for all times [7]. Using this variable time step method, no special algorithm [11] is required for high pressure (large ν_A, ν_B) simulations.

4.1. Simulation experiments

In the simulations reported here, the membrane is as shown in Fig. 1 but the membrane thickness L is varied from L=10 to L=100, and the membrane typically has a width of M=320 sites in the y-direction. For simplicity, the intrinsic rate k_x for jump attempts in the x-direction is used to set a dimensionless timescale for the simulations such that the unit of time is $\tau = 1/4k_x$. τ is the average residence time of a particle in an adsorption site of an isotropic square lattice.

In all the simulations reported here we have set the desorption rate equal to:

$$k_d = \frac{k_x}{100}, \tag{18}$$

to model the fact that jumping within the lattice is usually much faster than desorbing from the zeolite. Substituting in Eq. (15) we find that:

$$\frac{k_x}{k_d} = 100 = \frac{\alpha_3 \exp(-\beta E_x)}{\alpha_2 \exp(-\beta E_d)}. \tag{19}$$

If we set the prefactors on the right-hand side of this equation to be equal, we find that this corresponds to a

system temperature of:

$$T = \frac{E_d - E_x}{k_B \ln(k_x/k_d)}. \quad (20)$$

Using experimental values for silicalite-cyclohexane obtained by Magalhães et al. [19] for the heat of adsorption, E_d=17.5 kcal/mol, and the activation energy for transport diffusion in the fastest direction, E_x=11.5 kcal/mol, we find that the temperature of our simulations corresponds to T=656 K for cyclohexane in silicalite. This temperature was chosen primarily for simulation efficiency.

In addition to determining the ratio k_x/k_d, the temperature enters the theory and simulations through the timescale τ. Under certain assumptions this can be determined from data for cyclohexane in silicalite [19], yielding ca. $\tau=2\times10^{-7}$ s. This serves as the fundamental unit of time in our kinetic Monte-Carlo simulations. Using this unit of time, the durations of the TCP simulations reported here correspond to experimental times ranging from about 2 ms to about 10 s. In all the simulations we set $v_A=v_B$ with a value chosen from Eq. (2) to give a total occupancy at steady-state of θ_T=0.9 throughout the system. The physical pressure corresponding to this occupancy can be obtained from an isotherm at T=656 K.

The motivation for using the TCP boundary conditions shown in Fig. 1, is that we are interested in the equimolar counter-diffusion eigenmode of diffusion for lattices of finite size. At steady-state, the flux of species A is equal and opposite to that of species B, and the total occupancy θ_T is uniform throughout the lattice. This means that we can use Fick's law, Eq. (6), to determine the apparent diffusivity within the counter-diffusion eigenmode between any two adjacent columns. The terms in Eq. (6) then have the following interpretation: J_A is the transmembrane flux at steady-state, which is independent of lattice position; $\nabla\theta_A$ is replaced with the difference in A-occupancy between two adjacent columns i and $i+1$, separated by a distance $\Delta x\equiv1$ giving $(\theta_{A,i+1}-\theta_{A,i})/\Delta x$; and $D_A^+(i)$ is the local counter-diffusion eigenvalue for diffusion between columns i and $i+1$. By determining the diffusivity in this way, any system-size effects are immediately apparent as a deviation of the local apparent diffusivity from the bulk value.

5. Results

5.1. η=1 – Isotropic membrane

In the first simulation, we investigate the case of an isotropic lattice ($\eta\equiv k_y/k_x=1$). The system is therefore very similar to those presented previously [8], and serves as a valuable check on the vacancy algorithm developed above. The main difference in the present physical model is that we use a realistically slow desorption rate, with $k_d=k_x/100$, while in the earlier work we assumed that $k_d=k_x$.

Fig. 3 shows the time development of the concentration in selected columns of a membrane of thickness L=20 and M=320 sites in the y-direction. The data shown are the average values taken from an ensemble average of 50 independent simulation runs. The time period shown in Fig. 3 is the transient period. The subsequent time interval of length 45 000 time units was used to gather the steady-state data shown in Fig. 4. The horizontal lines shown in Fig. 3 are the steady-state values of the concentration in each of the columns. Corresponding data were obtained for

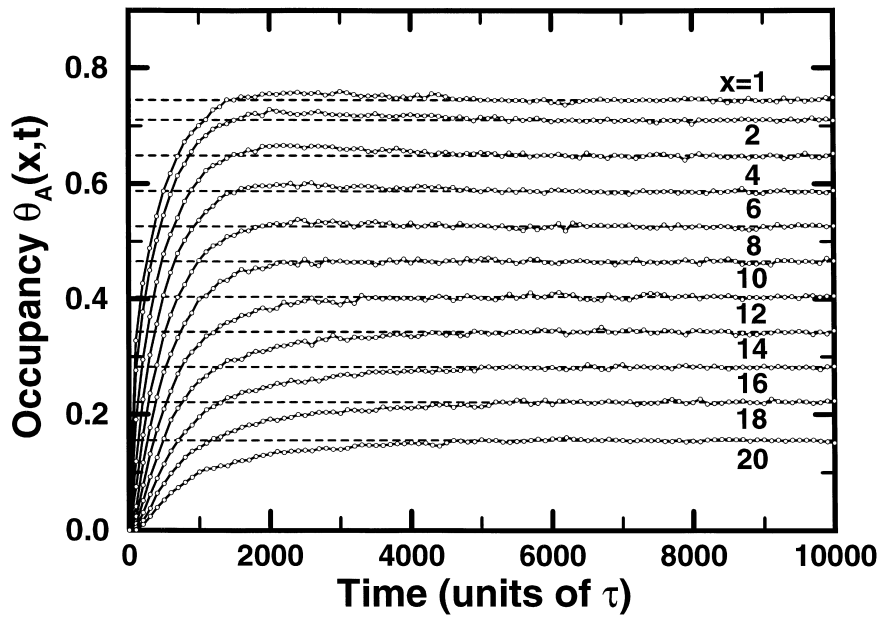

Fig. 3. Concentrations in selected columns, x, of an isotropic (η=1) membrane of thickness L=20, as a function of time during the transient portion of TCP simulations. Steady-state concentrations are shown as dashed lines.

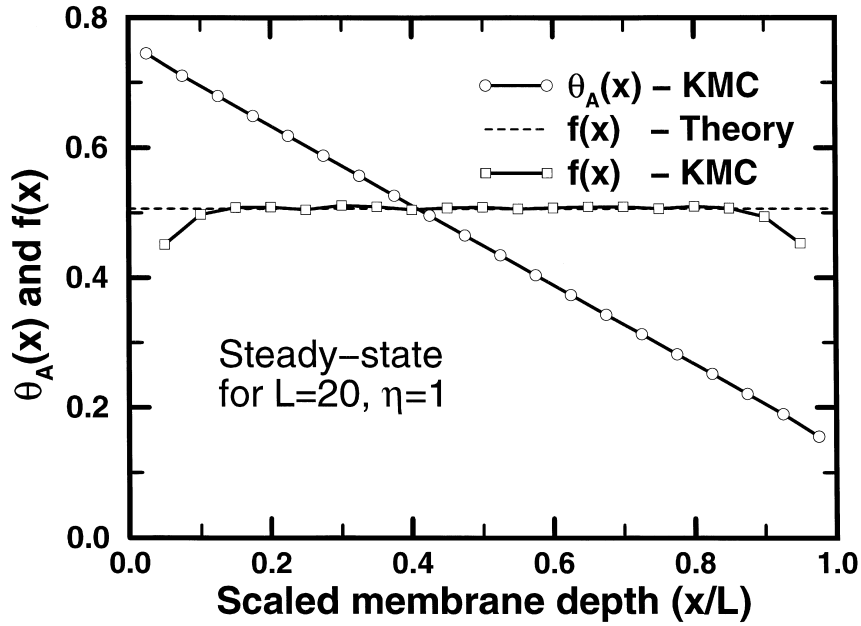

Fig. 4. Steady-state concentration profile, $\theta_A(x)$, and local diffusion correlation factor, $f(x)$, within an isotropic membrane of thickness $L=20$. Circles shown here correspond to dashed lines in Fig. 3. Local correlation factors agree well with theory for the isotropic membrane, shown as the dashed line.

all simulations reported here, and used to check that steady-state conditions had been reached.

The A-concentration near the inflow side of the membrane increases rapidly at short times and overshoots the steady-state value at intermediate times ($t\sim3000\tau$). This overshooting is a result of A-particles diffusing rapidly into the empty lattice before there is a significant number of B-particles near the A-inflow edge, and becomes more dramatic for small values of η. At a time of about $t=3000\tau$, the total concentration, θ_T, reaches its steady-state value throughout the lattice. The time required for this to occur is governed by the single-component transport diffusion coefficient, which governs the uptake of the total concentration, independently of the anisotropy η.

For times greater than $t\sim3000\tau$, diffusion within the membrane is governed solely by the equimolar counter-diffusion eigenmode. This eigenmode is slower than the single-component diffusivity and is the reason for the relatively slow approach to steady-state. While the A-concentrations near the left edge of the lattice overshoot their steady-state values, the A-concentrations near the right edge initially under-shoot their steady-state values. This feature is required by the symmetry of the TCP boundary conditions, where the A-concentration in column x is equivalent to the B-concentration in column $L-(x-1)$, so that $\theta_A(x)+\theta_B(x)=\theta_T(x)=\theta_T(L-(x-1))=\theta_A(x)+\theta_A(L-(x-1))$.

An initial test of the simulation method was to compare the simulation values of $\theta_T(x)$ with the predictions of the finite difference formulation (FDF) of diffusion theory for a single-component. The FDF for a single-component provides a numerically exact prediction for membranes of any thickness and for any value of the lattice anisotropy η. This simple comparison was performed as described in [7], and we found no statistically significant deviations between the simulation results and the FDF for single-component diffusion. It should be noted that choosing a "bad" random number generator can cause significant deviations. In the simulations reported here, we used the "ran2" random number generator described in [38], which produced no significant deviations from expected transport behavior.

The steady-state concentration values were obtained from the steady-state portion of the simulations ($t=10\,000\tau$ to $t=55\,000\tau$). From the outflow, an average flux through the lattice was determined, and this was used with the concentration gradient to determine the apparent diffusivity between two adjacent columns of the lattice according to

$$D_A^+(x) = \frac{J}{\theta_{A,x} - \theta_{A,x+1}}. \tag{21}$$

The apparent diffusivity in Eq. (21) was converted into a spatially local correlation factor using Eq. (9). A direct result of Eq. (21) at constant total occupancy is that whenever the correlation factor is constant in space, the steady-state concentration profile is linear. Hence, in what follows we will simply report the correlation factor.

We also compared the simulation results with the FDF for two-component diffusion. At steady-state, the FDF gives a linear concentration profile for species A, assuming that the correlation factor, and hence the counter-diffusivity, is uniform throughout the membrane. As we can see from Fig. 4, the diffusivity is equal to the theoretical value (dashed line) throughout most of the lattice. Counter-diffusion between the rows nearest to the edges gives slightly smaller values for the correlation factors than in the bulk, because the particles in the edge row change position more slowly than particles in the bulk.

In the absence of a general theory for the variation of the correlation factor near the edges of the lattice, we will make the approximation that the correlation factor is uniform throughout the lattice. Tahir-Kheli and El-Meshad [34] provide a theory for this spatially constant correlation factor (for $\eta>0$) that can be used to solve the FDF independently of the simulation data. The entire diffusion problem can thus be reduced to a set of finite difference equations as given above in Eqs. (10) and (11). Unlike the case for single-component diffusion, the FDF is not numerically exact for multi-component systems, but as we will see (vide infra), the errors are usually small and are reduced as the membrane thickness is increased.

5.2. Anisotropic membranes $\eta\neq1$

Figs. 5 and 6 summarize the results from a number of TCP computer experiments for membranes of various thicknesses and anisotropy values. The results discussed above for $\eta=1$ and $L=20$ are shown in Fig. 5, together with results for other anisotropies and membrane thicknesses. Apart from an edge effect increasing correlations in the two outermost layers, the bulk correlation factor is independent of lattice size. This length independence is characteristic of ''normal'' diffusion, where the diffusivity is a manifestation of localized phenomena that do not depend on system size. The results for membranes with $\eta=100$, 10, 1, 0.1, 0.01 are summarized in Fig. 5. We find that the counter-diffusivity depends strongly on the anisotropy of the membrane, but is independent of membrane thickness away from the edges, in an analogous manner to the isotropic membranes. Hence, for these values of the anisotropy, the system exhibits normal transmembrane counter-diffusion.

5.3. $\eta\gg1$ – Mean field theory

In the limit that $\eta\rightarrow\infty$, diffusion in the y-direction is much faster than in the x-direction, so that any correlations between jumps in the x-direction are washed out by the rapid motion in the y-direction. As a result, the correlation factor approaches unity for all concentrations as $\eta\rightarrow\infty$. We can see from Fig. 5 that for $\eta=100$, the correlation factor is already nearly equal to one. In this limit, the counter-diffusivity or self-diffusivity is given by:

$$D_S = D_0(1-\theta_T), \tag{22}$$

which is the result predicted by mean field theory. In the mean field theory, correlations are ignored so that the correlation factor has a value of unity. It is in this limit, $\eta\rightarrow\infty$, that the matrix diffusion theory outlined above reduces to the matrix theory of Qureshi and Wei [32]. This limit is also consistent with the Darken equation, eq. (1.30) in [1]:

$$D = D_s\left(\frac{\partial \ln f}{\partial \ln\theta}\right)_T. \tag{23}$$

For single-component Langmuirian systems, $D=D_0$ and Eq. (23) gives $D_S=D(1-\theta_T)=D_0(1-\theta_T)$, which is consistent with our results in the limit $\eta\rightarrow\infty$. Hence, in this limit the predictions of mean field theory, the Darken equation, Eq. (23), and our matrix formulation coincide. For finite values of η, Eq. (22) is in error by a factor inversely

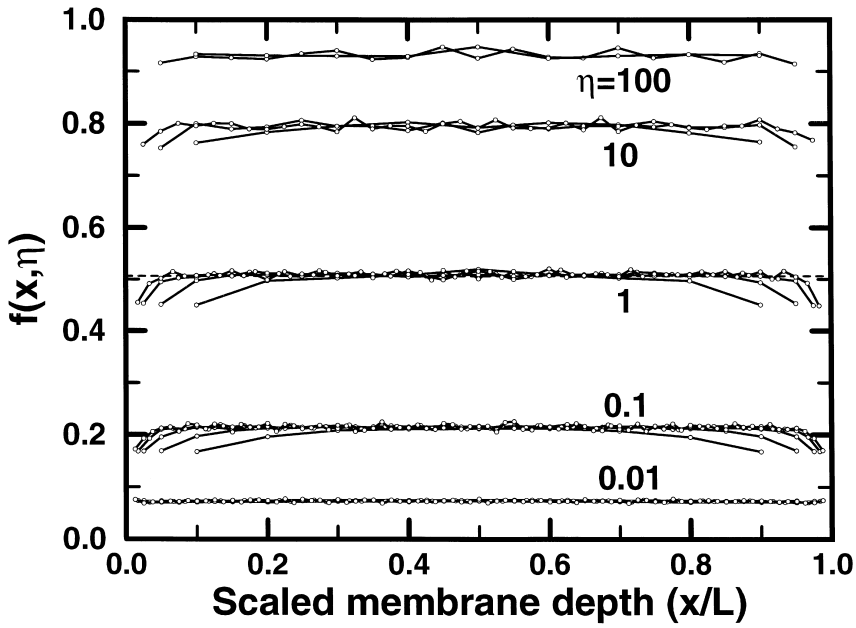

Fig. 5. Local diffusion correlation factors, $f(x,\eta)$, for anisotropic membranes of thicknesses $L=10$ to $L=100$ in the ''normal'' diffusion regime. The correlation factor for specified anisotropy, η, is independent of membrane thickness away from the edges. As η increases, correlation factors approach the mean field limit, $f=1$.

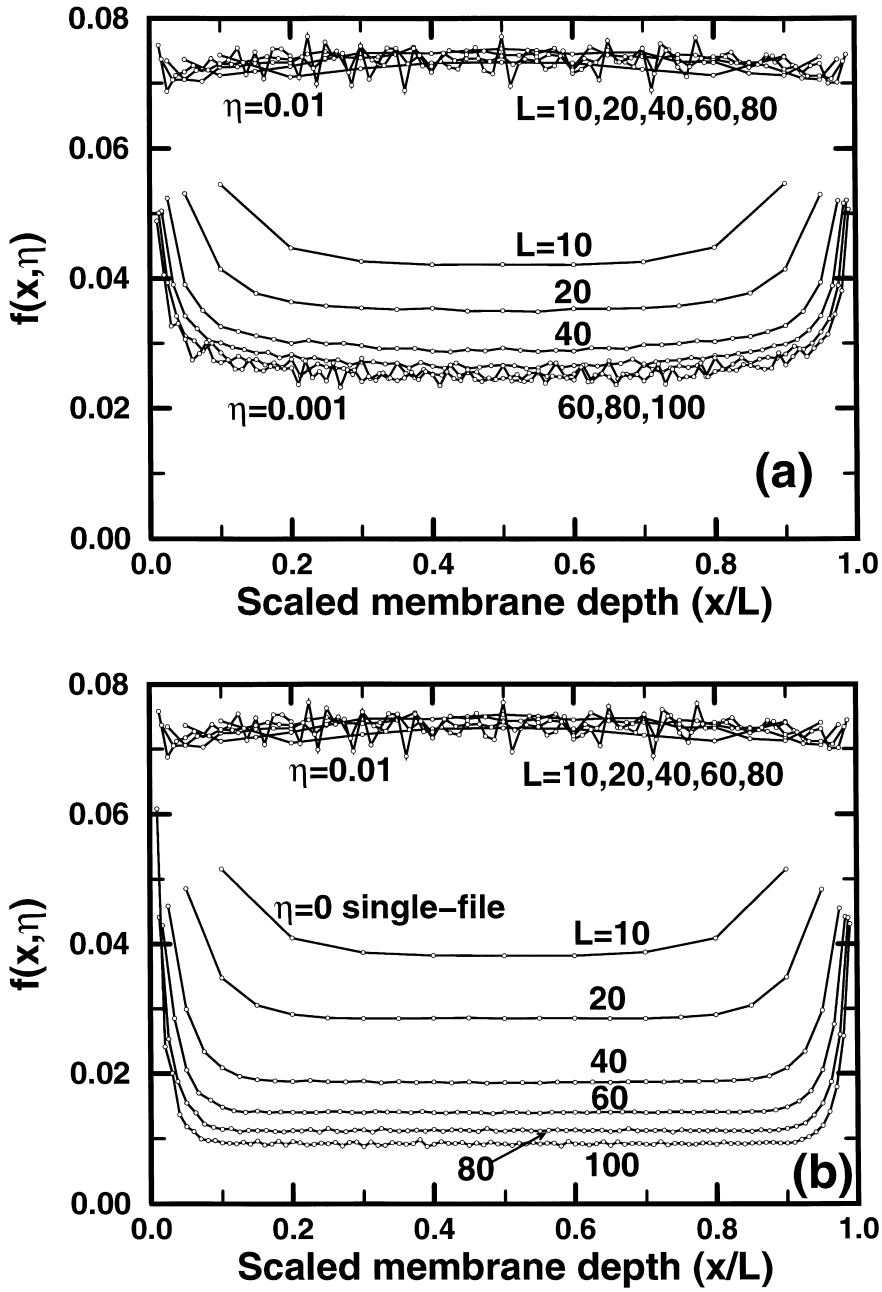

Fig. 6. Local diffusion correlation factors, $f(x,\eta)$, for highly anisotropic membranes ($\eta \ll 1$) of thicknesses $L=10$ to $L=100$. (a) $\eta=0.001$ membranes show single-file signature for $L<40$ and approach normal diffusion for $L>40$; (b) $\eta=0$, diffusivity is strictly single-file and decreases with L for all membrane thicknesses.

proportional to the correlation factor f, which, as we will show below, tends to zero for highly anisotropic lattices with $\eta \ll 1$.

We note that the large η limit discussed here involves a membrane for which diffusion in the fast lattice direction is not driven by any concentration gradient. This can only happen in a real system if the ends of the y-channels are not in contact with the external fluid, either by being blocked by the membrane's support, or in a free crystallite if unfavorable lattice terminations block the entrances to the edge sites in the y-direction. Otherwise, if the y-channels exchange particles with the external reservoirs, then the present $\eta=100$ case will be controlled by the faster diffusion in the y-direction, and thus be comparable to the situation here with $\eta=0.01$ (viz. exchanging the x- and the y-axis labels). In this case, the anisotropy justifies the use of a one-dimensional, flat-plate solution to the single-component diffusion problem along the fast-diffusion direction, as diffusion in the slow directions can be neglected. Magalhães et al. [19] found that just such a one-dimensional diffusion model quantitatively reproduced single-component transport diffusion of a number of sorbates in silicalite crystals,

with a concentration independent transport diffusivity as predicted by the Langmuirian model investigated here.

The $\eta>1$ anisotropic two-dimensional zeolite also provides an illustrative model showing how correlation effects can be reduced in zeolite systems with more than one particle jump rate. Consider a host–guest system such as Na-Y-benzene. Na-Y is a cage-type zeolite with four cation S_{II} adsorption sites per cage. Several calculations have shown that intra-cage benzene motion in Na-Y occurs on a timescale significantly shorter than inter-cage motion [40–43], the latter leading directly to self-diffusion through Na-Y. KMC simulation results for this system agree remarkably well with mean field theory, but no explanation for this agreement was available at the time. The intra-cage jump rate has little effect on the observed diffusion coefficient because intra-cage jumps, by themselves, cannot produce long range displacement. This is analogous to the jumps in the *y*-direction, which by themselves cannot produce transport diffusion in the *x*-direction of the anisotropic zeolite membrane. In analogy with the anisotropic membrane with $\eta>1$, the rapid, intra-cage jumps wash out correlations between inter-cage jumps, thereby giving diffusion in Na-Y modeled well by mean field theory.

5.4. $\eta \ll 1$ – Single-file versus normal diffusion

Fig. 6(a) and (b) show steady-state diffusion data for highly anisotropic membranes where diffusion in the transmembrane direction is much faster, i.e. $\eta \ll 1$. Although the $\eta=0.01$ diffusivities are independent of membrane thickness for all cases studied, the $\eta=0.001$ diffusivities depend on membrane thickness for thin membranes, but approach a constant limiting value for thicker membranes. This indicates that for small values of η, a relatively large lattice is required to reach the thick membrane limit, where the correlation length for diffusion is small compared to the system size. For thin membranes and small values of η, a diffusion mode with correlation lengths comparable to the membrane thickness, i.e. a global mode of diffusion, dominates. The extreme case of this occurs when $\eta=0$ and diffusion is strictly single-file. In this type of lattice there is no localized mechanism for diffusion [24], and the diffusion coefficient always depends on system size, as shown in Fig. 6(b) and Fig. 7.

We have developed a theory for TCP in high occupancy, single-file membranes that explains the limiting behavior, namely that $D_A^+ \to 0$ as the thickness of the membrane $L\to\infty$. Our theory, which will be reported in a forthcoming publication [24], gives the following expression for the counter-diffusivity as a function of total occupancy and membrane thickness, in the thick membrane limit:

$$D_A^+ = \frac{D_0(1-\theta_T)}{L\theta_T} \tag{24}$$

Very recently, this same expression was derived independently by Hahn and Kärger [23], for the long-time limit of the collective self-diffusion coefficient in a single-file membrane in the absence of driving forces. Qualitatively speaking, the factor $1/L$ arises because single-file counter-diffusion at high occupancies is a compound process, requiring a vacancy to traverse the entire length of the membrane to produce a particle displacement of one lattice spacing.

In comparing Fig. 6(a) and (b), we find that diffusion through thin membranes with $\eta=0.001$ is qualitatively similar to single-file diffusion, depending on membrane

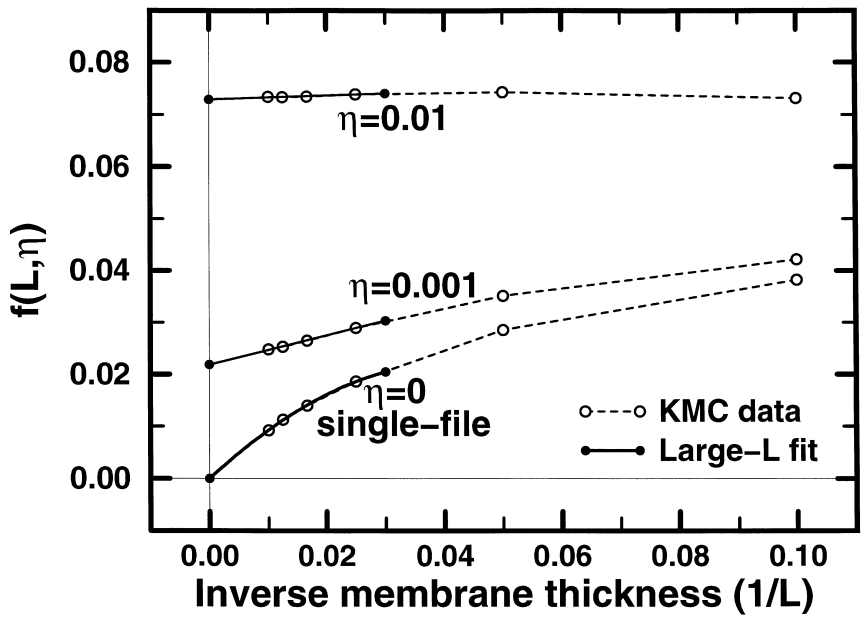

Fig. 7. The three types of membrane thickness dependence for the diffusivity: $\eta=0.01$, diffusivity independent of thickness; $\eta=0.001$, diffusivity approaches finite value as $L\to\infty$; and $\eta=0$, diffusivity tends to zero as $L\to\infty$. Open circles are simulation data and solid lines are fit to the $L\geq 40$ data points.

thickness in a similar manner. However, when the membrane is sufficiently thick for any $\eta>0$, normal diffusion takes over. In general, this occurs when the single-file diffusion coefficient becomes less than the limiting normal diffusion coefficient, which for $\eta=0.001$ occurs at a crossover thickness of about $L_c=30$. The condition that $\eta>0$ is similar to allowing particles in a one-dimensional tube to pass by each other [44]. This reduces the range of correlations among the particles from the width of the membrane to the length-scale required for exchange with a neighboring file.

Fig. 7 shows the bulk diffusivities for membranes with $\eta=0.01$, 0.001 and 0 as a function of inverse membrane thickness, $1/L$. As $L\to\infty$ and $1/L$ tends to zero, the diffusivities tend to a finite value so long as $\eta>0$. For $\eta=0.01$, the linear fit through the four data points ($L\geq 40$ shown in Fig. 7) has approximately zero slope. Thus, the correlation factor is essentially independent of membrane thickness and is governed by the normal diffusion mode.

For $\eta=0.001$, the correlation factor decreases with increasing length. The linear fit through the four data points ($L\geq 40$ shown in Fig. 7), has a non-zero intercept at infinite thickness ($1/L=0$). Thus, for sufficiently thick membranes, normal diffusion dominates and the diffusivity is independent of membrane thickness. The crossover thickness, L_c, for $\eta=0.001$ can be estimated from Fig. 7 as being $L_c\approx 30$, where the thick membrane normal diffusivity, as given by the intercept of the fit, equals the single-file diffusivity on the $\eta=0$ curve.

For $\eta=0$, the correlation factor decreases with increasing length. The non-linear fit through the four data points ($L\geq 40$ shown in Fig. 7) is consistent with the limiting form of Eq. (24), and will be discussed in more detail in a forthcoming publication. The most salient point is that the diffusivity tends to zero for thick membranes, and there is no region where the diffusivity is independent of membrane thickness.

6. Discussion

6.1. Permeation experiments

In this section, we define expressions that relate our simulation results to future TCP experiments using Langmuirian membranes when normal diffusion holds, i.e. $\eta>0$. Although we have only simulated relatively thin membranes, the diffusion theory is applicable to systems of arbitrary extent when normal diffusion dominates. In permeation or counter-permeation experiments, it is usually not possible to measure the intra-crystalline concentrations directly. Rather, only properties external to the membrane, such as the left and right reservoir partial pressures and the transmembrane flux, are experimentally accessible. If at steady-state we make the approximation that the local apparent diffusivity, D_A^+, is constant throughout the interior of the membrane, then the intra-membrane concentration profile is linear and we can write Fick's law in terms of the concentration difference between columns 1 and L, so that:

$$J_A = -D_A^+ \frac{\theta_{A,L} - \theta_{A,1}}{(L-1)}. \tag{25}$$

At the left and right edges of the membrane, respectively, the flux is given by:

$$J_A = v_{A,1}(1-\theta_{T,1}) - k_d\theta_{A,1} \quad \text{and}$$
$$J_A = k_d\theta_{A,L} - v_{A,L}(1-\theta_{T,L}), \tag{26}$$

where $v_{A,1}$ and $v_{A,L}$ are the constant insertion rates from the left and right fluid phases into columns 1 and L, respectively. For generalized steady-state TCP, the fluids on either side of the membrane may be A–B mixtures, and it is required that $v_{A,1}=v_{B,L}$, $v_{A,L}=v_{B,1}$ so that:

$$\theta_{T,1} = \theta_{T,L} = \theta_T = \frac{1}{1+(k_d/v_T)} \tag{27}$$

at steady-state, where $v_T=v_{A,1}+v_{B,1}$, and we can solve Eqs. (25)–(27) to obtain:

$$J_A = -\left[\frac{D_A^+(1-\theta_T)}{k_d(L-1)+2D_A^+}\right](v_{A,L}-v_{A,1}). \tag{28}$$

If the particle reservoirs are ideal gas mixtures, then the insertion rates, $v_{A,1}$ and $v_{A,L}$, can be replaced with terms proportional to the external partial pressures of species A. The permeance of the membrane is therefore proportional to the term in square brackets in Eq. (28).

When $k_d(L-1) \gg D_A^+$, diffusion through the membrane is much slower than desorption from the edges, so that transport through the membrane is diffusion-limited and Eq. (28) can be approximated by:

$$J_A \approx -\left[\frac{D_A^+(1-\theta_T)}{k_d}\right]\frac{(v_{A,L}-v_{A,1})}{L}, \tag{29}$$

where we have further assumed that $L\gg 1$. The term in square brackets in Eq. (29) is proportional to the permeability coefficient, which in this limit is independent of membrane thickness. Eq. (29) may also be derived by combining Eq. (25) with the assumption that the edge columns are in local thermodynamic equilibrium with the particle reservoirs, i.e. $\theta_{A,1}=v_{A,1}(1-\theta_T)/k_d$ and similarly for column L. This means that the assumption of local thermodynamic equilibrium as discussed in Section 5 is only valid when permeation is diffusion limited.

In the opposite limit, where transport through the membrane is sorption limited, i.e. $D_A^+ \gg k_d(L-1)$, we find that:

$$J_A \approx -(1-\theta_T)(v_{A,L}-v_{A,1})/2, \tag{30}$$

so that the permeance is proportional to the vacancy concentration $(1-\theta_T)=(1+(v_A/k_d))^{-1}$ and is independent of membrane thickness and the diffusivity. In this latter case we find that the permeability coefficient is proportional to

the membrane thickness L, rather than being independent of L (viz. Eq. (29)).

For the simulation results presented here, the ratio $k_d(L-1)/D_A^+$ ranges from about 1 for the $\eta=100$ simulation with $L=10$ to a value of about 1000 for the $\eta=0$ simulation with $L=100$. For a given system $D_A^+ \propto k_x$, and hence the ratio k_d/D_A^+ depends on temperature as indicated in Eq. (19). For silicalite-cyclohexane at room temperature, we find that the ratio $k_x/k_d \cong 23\,000$, and that the diffusion and sorption times are approximately equal for a membrane about $L=1000$ sites thick, corresponding to a membrane about 1 μm thick. This indicates that diffusion will not control permeation in real Langmuirian membranes at sufficiently low temperatures. This is only true if E_d is larger than E_x, which is the case considered in the simulations. However, it is possible although unlikely that E_d may be less than E_x in some Langmuirian host–guest systems. In this case, the ratio k_x/k_d will decrease with temperature so that the system will become more diffusion limited as temperature in decreased.

In actual TCP experiments, it may be convenient to have initial conditions different from those used in the computer experiments reported here. We suggest that in actual TCP experiments, the membrane be equilibrated with the same gas mixture on both sides of the membrane. At time $t=0$ the fluid on the left-hand side should be replaced with the desired mixture. The steady-state counter-permeation will be the same as discussed above, but the transient is now governed by the counter-diffusion eigenmode. This has the advantage that the diffusivity determined by the time-lag method [45] is now a true counter-diffusivity, which can be directly compared with the diffusivity obtained from the slope of the steady-state outflow. When $k_d(L-1) \gg D_A^+$, the time-lag diffusivity will equal the outflow slope diffusivity. If $k_d(L-1)$ is not significantly greater than D_A^+, then the time-lag diffusivity will be different from the steady-state slope diffusivity, and an estimate of k_d can be obtained by comparing them.

7. Conclusion

We have modeled the steady-state analog of self-diffusion, tracer counter-permeation (TCP), in zeolite membranes of finite thickness via kinetic Monte-Carlo methods. The membrane and diffusing particles have a Langmuir-type isotherm. We performed our TCP simulations near the saturation point of the membrane lattice. The intra-lattice diffusivities were determined from local concentration gradients and the steady-state transmembrane flux using Fick's law. The influences of diffusion anisotropy and membrane thickness were investigated for this Langmuirian host–guest system with a desorption rate that was realistically slow compared to the diffusion jump rate.

We identified two mechanisms for counter-diffusion at high occupancy, depending upon the value of an anisotropy parameter, $\eta \equiv k_y/k_x$, where k_x is the jump rate coefficient along the transmembrane direction, and k_y is that normal to the transmembrane direction. The first is a "normal" counter-diffusion mechanism, in which diffusion is a localized phenomenon, occurring with a correlation length significantly less than the membrane thickness. The counter-diffusivity is constant throughout the membrane and is independent of membrane thickness. As η approaches infinity, correlations in the transmembrane direction are washed out by rapid motion in the y-direction, and the counter-diffusivity approaches mean field predictions. For decreasing values of η, motion in the transmembrane direction becomes more correlated, which decreases the counter-diffusivity.

The other mechanism is a "single-file" counter-diffusion mechanism, in which diffusion is a global phenomenon, occurring with a correlation length equal to the membrane thickness. In the single-file mechanism, the diffusivity is constant throughout the membrane and decreases with membrane thickness. In the extreme case, $\eta=0$ and motion in the y-direction is not possible. Counter-diffusion through the membrane is then strictly single-file for all membrane thicknesses and becomes inversely proportional to membrane thickness in the thick-membrane limit.

For highly anisotropic membranes satisfying $0<\eta \ll 1$, there is a crossover thickness, L_c, between the single-file and normal diffusion modes. For membranes thinner than L_c, transport is achieved primarily by the global, single-file mechanism. As the membrane thickness is increased, diffusion produced by the single-file mechanism slows, until for membranes thicker than L_c, transport is achieved primarily by normal diffusion. The normal diffusion mechanism dominates in all sufficiently thick membranes with $\eta \neq 0$.

We have presented a general theory for tracer diffusion in Langmuirian host–guest systems, based on a matrix form of Fick's law. This theory also includes a finite difference formulation that can be applied to a finite difference grid corresponding to the adsorption sites of the zeolite, and includes the adsorption and desorption rates at exposed lattice edges. Transport problems with boundary and initial conditions different from those considered above can be solved using the theory. For example, self-diffusion is equivalent to equimolar counter-diffusion at long times; the tracer zero-length column (TZLC) technique corresponds to a transient counter-diffusion problem; and TCP is a steady-state problem within the counter-diffusion eigenmode.

The theory exhibits a kinetic limitation at the exposed lattice edges, which may prevent the edge sites from reaching local thermodynamic equilibrium with the external phase even after steady-state is achieved, if the "diffusion time" is not significantly longer than the "sorption time." The diffusion time through a membrane of thickness L is approximately given by L^2/D where D is the counter-diffusivity. The sorption time is given by L/k_d, where k_d is the desorption coefficient. When the diffusion time is much

longer than the sorption time, transmembrane permeation is diffusion-limited and the transport can be modeled as a diffusion problem with constant-concentration boundary conditions, giving a membrane permeability coefficient that is independent of thickness. When the sorption time is much longer than the diffusion time, transmembrane permeation is sorption-limited and the membrane permeability coefficient depends upon membrane thickness. In the sorption-limited case, the permeance is the quantity that is independent of thickness. The lack of local thermodynamic equilibrium at the edges can have a significant effect on the overall transport problem, even in relatively large systems. For example, using the local thermodynamic equilibrium assumption, the counter-permeance of a 0.1 μm silicalite membrane to cyclohexane is overestimated by about an order of magnitude.

In future work we will present a theory for single-file tracer counter-permeation in Langmuirian membranes of arbitrary thickness. Extension of the simulation technique to non-identical multicomponent systems is straightforward. However, the theory becomes more complex because the eigenmodes of the diffusion matrix no longer correspond to the single component transport- and self-diffusivities [25,32]. Further development of the model to include more complicated lattice structures and sorbate–sorbate interactions is planned, to investigate the effects of these changes on the base model presented here.

Acknowledgements

The authors thank Dr. Fabien Jousse for many stimulating discussions. S.M.A. thanks the National Science Foundation (CHE-9616019 and CTS-9734153) and the National Environmental Technology Institute for generous funding.

References

[1] J. Kärger, D.M. Ruthven, Diffusion in Zeolites and Other Microporous Solids, Wiley, New York, 1992.
[2] N.Y. Chen, T.F. Degnan, C.M. Smith, Molecular Transport and Reaction in Zeolites, VCH Publishers, New York, 1994.
[3] J. Weitkamp, in: G. Olhmann, J.C. Vedrine, P.A. Jacobs (Eds.), Catalysis and Adsorption by Zeolites, Elsevier, Amsterdam, 1991, p. 21.
[4] P. Demontis, G.B. Suffritti, Chem. Rev. 97 (1997) 2845.
[5] C. Saravanan, F. Jousse, S.M. Auerbach, Phys. Rev. Lett. 80 (1998) 5754.
[6] D. Theodorou, J. Wei, J. Catal. 83 (1983) 205.
[7] P.H. Nelson, A.B. Kaiser, D.M. Bibby, J. Catal. 127 (1991) 101.
[8] P.H. Nelson, J. Wei, J. Catal. 136 (1992) 236.
[9] E.J. Maginn, A.T. Bell, D.N. Theodorou, J. Phys. Chem. 97 (1993) 4173.
[10] S. Fritzsche, R. Haberlandt, J. Kärger, Z. Physik. Chem. 189 (1995) 211.
[11] C. Rödenbeck, J. Kärger, K. Hahn, J. Catal. 157 (1995) 656.
[12] M.C. Lovallo, M. Tsapatsis, AICHE J. 42 (1996) 3020.
[13] W.J.W. Bakker, F. Kapteijn, J. Poppe, J.A. Moulijn, J. Membr. Sci. 117 (1996) 57.
[14] C.D. Baertsch, H.H. Funke, J.L. Falconer, R.D. Noble, J. Phys. Chem. 100 (1996) 7676.
[15] A.J. Burggraaf, Z.A.E.P. Vroon, K. Keizer, H. Verweij, J. Membr. Sci. 144 (1998) 77.
[16] A.W. Adamson, Physical Chemistry of Surfaces, 5th ed., Wiley, New York, 1990.
[17] R. Kutner, Phys. Lett. A 81 (1981) 239.
[18] D.M. Shen, L.V.C. Rees, J. Chem. Soc., Faraday Trans. 91 (1995) 2027.
[19] F.D. Magalhães, R.L. Laurence, W.C. Conner, J. Phys. Chem. B 102 (1998) 2317.
[20] K. Hahn, J. Kärger, V. Kukla, Phys. Rev. Lett. 76 (1996) 2762.
[21] V. Gupta, S.S. Nivarthi, D. Keffer, A.V. McCormick, H.T. Davis, Science 274 (1996) 164.
[22] S. Brandani, Z. Xu, D. Ruthven, Microporous Mater. 7 (1996) 323.
[23] K. Hahn, J. Kärger, J. Phys. Chem. B 102 (1998) 5766.
[24] P.H. Nelson, S.M. Auerbach, J. Chem. Phys. 110 (1999) 9235.
[25] K.W. Kehr, K. Binder, S.M. Reulein, Phys. Rev. B 39 (1989) 4891.
[26] A.J. Slavin, P.R. Underhill, Am. J. Phys. 54 (1984) 376.
[27] A.R. Paravar, D.T. Hayhurst, in: D. Olson, A. Bisio (Eds.), Proceedings of the Sixth International Zeolite Conference, Butterworths, London, 1984, p. 217.
[28] D.T. Hayhurst, A.R. Paravar, Zeolites 8 (1988) 27.
[29] D. Prinz, L. Reikert, Ber. Bunsenges. Phys. Chem. 90 (1986) 413.
[30] W.R. Qureshi, J. Wei, J. Catal. 126 (1990) 147.
[31] J. Xiao, J. Wei, Chem. Eng. Sci. 47 (1992) 1143.
[32] W.R. Qureshi, J. Wei, J. Catal. 126 (1990) 126.
[33] K. Binder, Rep. Prog. Phys. 60 (1997) 487.
[34] R.A. Tahir-Kheli, N. El-Meshad, Phys. Rev. B 32 (1985) 6166.
[35] P.H. Nelson, T.A. Hatton, G.C. Rutledge, J. Chem. Phys. 107 (1997) 1269.
[36] E. de Vos, A. Bellemans, Macromolecules 8 (1975) 651.
[37] K.A. Fichthorn, W.H. Weinberg, J. Chem. Phys. 95 (1991) 1090.
[38] W.H., Press, S.A. Teukolsky, W.T. Vettering, B.P. Flannery, Numerical Recipes in C, the Art of Scientific Computing, 2nd ed., Cambridge University Press, New York, 1992.
[40] S.M. Auerbach, N.J. Henson, A.K. Cheetham, H.I. Metiu, J. Phys. Chem. 99 (1995) 10600.
[41] F. Jousse, S.M. Auerbach, J. Chem. Phys. 107 (1997) 9629.
[42] T. Mosell, G. Schrimpf, J. Brickmann, J. Phys. Chem. B 101 (1997) 9476.
[43] T. Mosell, G. Schrimpf, J. Brickmann, J. Phys. Chem. B 101 (1997) 9485.
[44] D.S. Sholl, K.A. Fichthorn, J. Chem. Phys. 107 (1997) 4384.
[45] J. Crank, The Mathematics of Diffusion, 2nd ed., Oxford University Press, Oxford, 1978.